CHEMICAL ENGINEERING TRANSACTIONS Volume 18, 2009
Editor Jiří Klemeš
 ISBN 978-88-95608-04-4 ISSN 1974-9791
DOI: 10.3303/CET0918117

Kinetic parameters estimation for precipitation using continuous approximation functions and genetic algorithms

Raluca Isopescu and Vasile Lavric
University Politehnica of Bucharest, Department of Chemical Engineering
RO 011061, 1-7 G. Polizu Street, Bucharest, Romania

The present work presents the modeling and kinetic parameters estimation for the semi-continuous precipitation process of calcium carbonate. The parameters estimation was performed using genetic algorithms (GA) throughout minimization of two objective functions: (i) the norm of the residual *experimental particle size distribution - computed data* and (ii) the norm of the *population balance* (PB) *residual* computed with the estimated kinetic parameters. The PB equation takes into account homogenous nucleation, size dependent growth and agglomeration as the governing mechanisms of precipitation. The theoretical particle size distribution (PSD) was approximated by a continuous parameterized functional built up from piece-wise time-weighted exponential functions having time and crystal size as independent variables. The parameters of the functional were estimated together with the aforementioned kinetic parameters. The methodology was applied using data obtained for the semi-continuous precipitation of $CaCO_3$ by the chemical reaction between equivalent volumes of $CaCl_2$ and K_2CO_3 solutions.

1. Introduction

The precipitation of sparingly soluble salts as a result of a homogeneous reaction in semi-batch crystallizers is a common procedure in industrial fabrications of chemicals. The homogeneous nucleation induced by the fast chemical reaction generates new particles all over the reaction time. The PB technique is widely used to model crystallization and precipitation processes as it captures the changes in PSD seen as the result of four basic processes acting upon the particles within a control volume: birth, growth, break-up and agglomeration (Barbier et al., 2009). Considering the characteristic particle size (denoted by L) as the internal coordinate of the solid phase that is formed, the population balance equation (PBE) for the dynamic regime can be written as:

$$\frac{\partial n(L,t)}{\partial t} + \frac{\partial\left[G(L,t)\cdot n(L,t)\right]}{\partial L} = r(n,L,t) \tag{1}$$

where $n(L,t)$ is the population density function, $G(L,t)$ is the growth rate function and $r(n,L,t)$ is a complex functional, with integral terms, representing generation and/or death functions that model nucleation, agglomeration and/or breakage processes.

Please cite this article as: Isopescu R. and Lavric V., (2009), Kinetic parameters estimation for precipitation using continuous approximation functions and genetic algoritms, Chemical Engineering Transactions, 18, 719-724 DOI: 10.3303/CET0918117

2. Experimental

The precipitation was carried on in a 0.5 L crystallizer at 30 ^{0}C. A volume of 0.250 L of 0.1 M $CaCl_2$ solution was initially placed in the vessel. An equivalent volume of 0.1 M K_2CO_3 solution was added at a flowrate of 1 L/h. Suspension samples were taken at different feeding moments and PSD was measured, in terms of mass distribution, on a laser beam particle analyzer. The precipitated solid phase was identified as pure calcite according to FT-IR spectra analysis.

The population density function *n(L)* was computed from the experimental PSD using the common transformation of first order approximation:

$$n(L) = \frac{\left[M(L_i) - M(L_{i-1})\right] \cdot m_T}{\overline{L_i}^3 \cdot \rho_s \cdot k_v \cdot (L_i - L_{i-1})} \tag{2}$$

where *M(L)* is the cumulative mass distribution, m_T is the solid mass in the unit volume of suspension, evaluated from overall mass balance, ρ_s is the density of calcite and k_v the volumetric shape factor which, for calcite, takes the value of 1.

3. Mathematical model

3.1 Kinetic model

The precipitation happens due to a supersaturation generated by the chemical reaction:

$$CaCl_2 + K_2CO_3 \rightarrow CaCO_3 + 2KCl \tag{3}$$

The resulted calcium carbonate has a very low solubility and precipitation occurs almost instantaneously. The relative supersaturation is computed according to the general mass action law for the ionic reactions and assuming perfect mixing of the reaction system:

$$S = \sqrt{\frac{\left[Ca^{2+}\right] \cdot \left[CO_3^{2-}\right]}{K_{sp}}} \tag{4}$$

where the solubility constant, K_{sp}, has the value of $3.4 \cdot 10^{-9}$ $(mol/L)^2$ for calcite. The concentration of Ca^{2+} and CO_3^{2-} ions are calculated from mass balances at the given flowrate. The supersaturation increases rapidly during the first 10 s from the addition of the second reagent, then decreases while nucleation and crystallization of the solid phase progress and calcium ions are consumed. The assumed crystallization mechanisms consist of primary and secondary processes (solid phase homogenous nucleation and crystal growth for the former, agglomeration for the latter). The overlapping o these mechanisms, all along the reaction period, generates specific PSD shapes, with steep variations especially in the range of small particles. The kinetic models assumed for each implied mechanism reflects the dependency of its specific rate on supersaturation.

$$B^0(t) = k_B \left[S(t)\right]^{n_B} \tag{5}$$

$$G(L,t) = G_0(t) \cdot (1 + a \cdot L)^b \tag{6}$$

$$G_0(t) = k_G \cdot \left[S(t)\right]^{n_G} \tag{7}$$

where $B^0(t)$ is the nucleation rate depending only on supersaturation while $G(L,t)$ is the crystal growth rate depending on the crystal characteristic length, L. $G_0(t)$ is the growth rate at zero nucleus-size, while a and b are the parameters of the size dependent

growth model.

3.2 Population balance equation

The general PBE for precipitation describes the time and size variation of the number based density function $n(L,t)$ when different overlapping mechanisms are active:

$$\frac{1}{V(t)}\frac{\partial\left[n(L,t)\cdot V(L)\right]}{\partial t}+\frac{\partial\left[G(L,t)\cdot n(L,t)\right]}{\partial L}=B^{0}\delta(L-L_{0})+B(L,t)-D(L,t) \tag{8}$$

where *V(t)* is the reaction volume while *B(L,t)* and *D(L,t)* represent the birth and death functions characterizing the agglomeration process.

$$B(L,t)=\frac{1}{2}\int_{0}^{L}\beta(L,y,t)\cdot n(L-y,t)\cdot n(y,t)\cdot dy \tag{9}$$

$$D(L,t)=\int_{0}^{\infty}\beta(L,y,t)\cdot n(L,t)\cdot n(y,t)\cdot dy \tag{10}$$

where β is the agglomeration kernel representing the rate constant for the agglomeration process. This constant can be also expressed as a compound function containing the size dependency and the influence of supersaturation:

$$\beta(L,y,t)=\beta_{0}(t)\cdot\beta^{s}(L,y) \tag{11}$$

$$\beta^{s}(t)=k_{\beta}\cdot\left[S(t)\right]^{n_{\beta}} \tag{12}$$

At high supersaturation, bridges can form between particles that collide and larger particles could be generated. This is the reason why the time dependency of the agglomeration kernel is expresses as a function of supersaturation. As the size dependent crystal growth stands for higher growth rate for larger particles and thus can cover also the agglomeration of large particles with newly formed nuclei, the agglomeration kernel used in the present work includes a correction size dependent factor that increases the contribution of the agglomerates formed throughout the collisions between medium particles, curbing the aforementioned effect.

The PBE was rendered dimensionless by using the notations: $\xi=L/L^{\max}$, $\tau=t/\bar{t}$ and $\upsilon(\xi,\tau)=n(\xi,\tau)/n^{\max}$, where $L^{\max}$ is the maximum obtained crystal size, $\bar{t}=V_{0}/F_{V}$ is the crystallizer time-scale, defined as the ratio between the volume V_0 of the reagent initially added in the precipitation vessel and F_V the volumetric flowrate, while $n^{\max}$ is the highest value of the population density function. With these notations, the dimensionless population balance equation becomes:

$$\begin{aligned}\Psi(\xi,\tau)=&\frac{\partial\upsilon(\xi,\tau)}{\partial\tau}+\frac{\upsilon(\xi,\tau)}{(1+\tau)}+G^{*}(\xi,\tau)\cdot\left[\frac{\partial\upsilon(\xi,\tau)}{\partial\xi}+\frac{\upsilon(\xi,\tau)\cdot a\cdot b\cdot L^{\max}}{1+a\cdot L^{\max}\cdot\xi}\right]-B^{*}(\tau)-\\&-\beta^{*}(\tau)\cdot\left[\int_{0}^{\xi}\beta_{\xi\zeta}(\xi,\zeta)\cdot\upsilon(\xi-\zeta,\tau)\cdot\upsilon(\zeta,\tau)d\zeta-2\cdot\upsilon(\xi,\tau)\int_{0}^{1}\beta_{\xi\zeta}(\xi,\zeta)\cdot\upsilon(\zeta,\tau)d\zeta\right]=0\end{aligned} \tag{13}$$

The significance of *B**, *G** and β* is the following:

$$B^{*}(\tau)=\frac{B^{0}(\tau)\cdot\delta(\xi-\xi_{0})\cdot\bar{t}}{n^{\max}} \tag{14}$$

$$G^*(\xi,\tau)=\frac{G^0(\tau)\cdot\left(1+a\cdot L^{\max}\cdot\xi\right)\cdot\overline{t}}{L^{\max}} \tag{15}$$

$$\beta^*(\tau)=\frac{\beta_0(\tau)\cdot\overline{t}\cdot n^{\max}\cdot L^{\max}}{2} \tag{16}$$

The function chosen for the correction factor to reflect the particle size dependency of the agglomeration kernel, as mentioned before, is:

$$\beta^*_{\xi\zeta}(\xi,\zeta)=\sqrt{\zeta}\cdot\left(1-\zeta^2\right)\cdot\sqrt{\xi}\cdot\left(1-\xi^2\right) \tag{17}$$

The mathematical model defined by the equations (13-17) is characterized by the following parameters that have to be estimated following an appropriate optimization procedure: k_B, n_B, k_G, n_G, a, b, k_β, n_β.

3.3 Continuous functional approximation of the population density function

The experimental distribution data measured after 480 s and 960 s (900 s is the time corresponding to the end of the second reagent addition), are presented in Figure 1. The shape of this curves, as well as the nature of population balance equation are good reasons to assume for the dimensionless population density function a continuous parameterized functional built up from piece-wise time-weighted exponential functions having time and crystal size as independent variables. We suggested a functional of the type:

$$f(\xi,\tau)=\exp\left[\left(a_f+b_f\cdot\tau\right)+\left(c_f+d_f\cdot\tau\right)\mathrm{e}^{\left(e_f+f_f\cdot\tau\right)\cdot\xi}+\left(g_f+h_f\cdot\tau\right)\mathrm{e}^{\left(i_f+j_f\cdot\tau\right)\cdot\xi}\right] \tag{18}$$

This functional can approximate the experimental distribution, when appropriate values for the function's parameters (a_f, b_f, c_f, d_f, e_f, f_f, g_f, h_f, i_f, and j_f) are used. Therefore, a suitable optimization procedure shell be used in order to search for both sets of parameters, corresponding to the functional mimicking the experimental distribution, and to the crystallization mechanisms, respectively.

3.4 Objective functions and optimization procedure

The validation of crystallization mechanisms assumed and the estimation of corresponding kinetic parameters is realized by formulating a two-objective function:

$$F1=\min\sqrt{\sum_{i=1}^{N}\left[\ln(f_i)-\ln(v_i)\right]^2} \tag{19}$$

$$F2=\min\sqrt{\sum_{i}^{N}\psi_i(\xi,\tau)^2} \tag{20}$$

where N is the total number of experimental points describing the time profiles of the crystal size distribution.

The first objective function stands for the goodness of fit with the experimental distribution curves while the second objective function reflects the residual of the population balance equation. Minimizing the second objective function the values of kinetic parameters that verify the PBE will be estimated.

The minimization was carried out using an improved version of GA (Răducan et al., 2004) which is expected to give better results due to its capability to explore a wide range of parameter variation and find the global optimum even for multimodal objective functions which is the case when 8 kinetic parameters and 10 functional parameters are to be simultaneously identified.

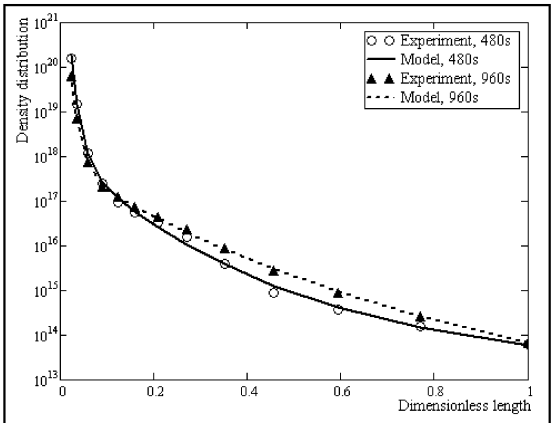

Figure 1. Experimental and computed population density function

The implemented GA have several general and specific features: *(a)* the direct storage of parameters on chromosome-like structure, for a faster retrieval and processing; the restrictions are dealt with simply eliminating the individuals violating them; *(b)* the optimal value is searched for within a group of candidate solutions, assimilated to a population; *(c)* the vector objective function is used to compute fitness values, for each individual, measuring its adequacy; several genetic operators (selection, crossover, mutation and cloning), are used to create new offspring from best fitted individuals; *(d)* when a large part of the population has too many bad fitted individuals, preventing them to participate at multiplication, apply cloning by selecting randomly from the better fitted individuals and *(e)* if elitism is sought, the individuals from the new population not born through crossover are generated randomly around the best fitted individual, using a shrinking standard deviation (Răducan et al., 2004).

4. Results and discussions

The mathematical model was solved for a time period of 960 s and the experimental data obtained after 480 s and 900 s were used in the optimization stage. The procedure defined in this work avoids the integration of the integro-differential equation representing the PB, since the functional is differentiated analytically and then introduced into the PB equation. Solving the PBE using the normal methodologies implies that the derived system of ODEs often becomes stiff, with the pending numerical difficulties, due to the continuous nucleation process and the overlapping of agglomeration (Jones et al, 2005). On the other hand any numerical approximation of the PB may introduce significant computational errors. We hope that using a continuous functional to approximate PSD will avoid such difficulties.

Several iterations were necessary to isolate the best parameters' intervals. Since the experimental PSD profiles are affected by errors (measurements, lumping in classes, passing from mass to number distributions), the two norms constituting the vector objective function should behave opposite during minimization: when the functional approaches too much the experimental PSD, the errors will drive the PB equation from closing. On the other hand, the mechanisms acting during the crystallization are more than what we took under consideration in our model (but they are reflected in the values of experimental PSD), so a complete closure of the PB equation will increase too much the distance between the theoretical and experimental PSDs. Consequently, a Pareto front will appear during optimization, the evolution of which is depicted in Figure 2. It may be noticed that the Pareto front evolves towards lower values for both objective functions. As can be seen analyzing the solution set, an increase in the precision of experimental

data approximation by the computed distribution function leads to a set of kinetic parameters that verify less satisfactory the PBE. As Figure 2 shows, function F1 cannot take smaller than 2.5 values while the objective function F2 decreases as the iterative process proceeds and the Pareto front becomes more restrained. For the final values of the optimized parameters the obtained continuous function gives a very good approximation of the experimental curves (Figure 1).

Table 1 Kinetic parameters

k_B, no·m^{-3}s^{-1}	n_B	k_G, m·s^{-1}	n_G	a, m^{-1}	b	k_β, m^3·s^{-1}	n_β
$3.22 \cdot 10^{15}$	0.037	$9.35 \cdot 10^{-10}$	0.944	$1.02 \cdot 10^{6}$	0.910	$1.58 \cdot 10^{-18}$	1.490

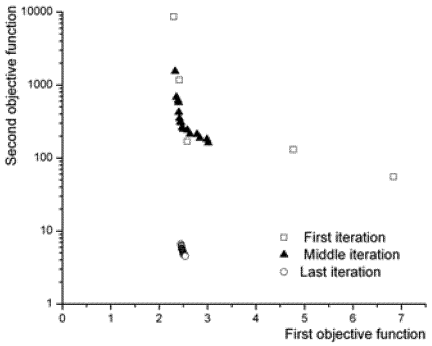

Figure 2. Variation of objective function F2 vs. objective function F1

The values of the optimized kinetic parameters (see Table 1) show that under the experimental conditions nucleation is dominant and the increase in crystal size is mainly due to the size dependent crystal growth mechanism. The fact that F2 has a rather high value means that not all the computed PSD are good solutions of the PBE. This might prove that the mechanisms considered in modelling the crystallization process should be improved: agglomeration kernel and heterogeneous nucleation which implies a dependency on the suspension's density.

5. Conclusions

The procedure defined in the present work, which still needs refinements, enabled us to obtain with reasonable computing efforts a good insight of the precipitation process, to validate the mechanisms implied and to estimate the kinetic parameters.

References

Babier E., Coste M., Genin A., Jung D., Lemoine C., Logette S., Muhr H., 2009, Simultaneous determination of nucleation and crystal growth kinetics of gypsum, Chem. Eng. Sci., 64, 363-369.

Jones, A., Rigopoulos, S., Zauner R., 2005, Crystallization and precipitation engineering, Comp. Chem. Eng., 29, 1159-1166.

Răducan, O., Lavric, V., Woinaroschy, A., 2004, Time Optimal Control of Batch Reactors through Genetic Algorithms, Rev. Chim., 55(8), 638-642.

Acknowledgments: The research wok was supported by The Romanian Ministry of Education and Research through "National Program II" Project no. 22116/2008